International Journal of Mass Spectrometry 305 (2011) 116–119

Contents lists available at ScienceDirect

International Journal of Mass Spectrometry

journal homepage: www.elsevier.com/locate/ijms

High mass accuracy and resolution facilitate identification of glycosphingolipids and phospholipids

Huan He[a], Mark R. Emmett[a,*,1], Carol L. Nilsson[a,2], Charles A. Conrad[b], Alan G. Marshall[a,**]

[a] Ion Cyclotron Resonance Program, National High Magnetic Field Laboratory, Florida State University, 1800 E. Paul Dirac Drive, Tallahassee, FL 32310, USA
[b] The University of Texas M.D. Anderson Cancer Center, Department of Neuro-Oncology, Houston, TX 77030, USA

ARTICLE INFO

Article history:
Received 14 July 2010
Received in revised form 7 October 2010
Accepted 13 October 2010
Available online 20 October 2010

This article is dedicated to Professor Catherine Costello, as part of this special issue of the *International Journal of Mass Spectrometry*.

Keywords:
Kendrick mass
FT-ICR MS
Fourier transform ion cyclotron resonance
Lipidomics
Isotopic fine structure
3-*O*-Sulfoglucuronylparagloboside (SGPG)

ABSTRACT

Natural lipid profiling can improve our current understanding of disease mechanism in a systems biology approach combining genomics, proteomics, and phenotypic changes. However, lipid profiling is complicated by the >10,000 combinations of polar head group, hydrocarbon chain length and degree of unsaturation/hydroxylation, and glycan composition and branching pattern. Here, we show how LC separation coupled with high resolution Fourier transform ion cyclotron resonance mass analysis can quickly narrow down the possible phospholipid and glycosphingolipid compositions. That approach necessitates resolution of mass differences as small as 1.8 mDa [$^{12}C_2{}^{13}C_1N_1$ (51.0064 Da) vs. H_3O_3 (51.0082 Da)] in phospholipids and 1.6 mDa [$^{13}C_2S_1H_2$ (59.9944 Da) vs. N_2O_2 (59.9960 Da)] in glycosphingolipids. For novel/unknown lipid species, high mass accuracy based Kendrick mass defect analysis enables quick grouping of related lipid species for subsequent tandem MS structural characterization. For sulfur-containing lipid species, high mass resolution can reveal isotopic fine structure to verify assignment.

1. Introduction

Lipid profiling is receiving increasing attention because lipids play important roles in cellular functions and are involved in cellular signal cascades. Recent reviews illustrate progress in the field of lipidomics and its contribution to the improved understanding of cellular biochemistry and systems biology [1,2]. Various phospholipids, previously considered as mere structural support, function as secondary messengers. For example, phosphorylation of phosphatidylinositol (PI) by phosphoinositide 3-kinases (PI3Ks) produces phosphatidylinositol 3,4-bisphosphate ($PI(3,4)P_2$) or phosphatidylinositol 3,4,5-trisphosphate ($PI(3,4,5)P_3$), which can regulate complex downstream signaling networks, including those involved in cell cycle, survival, and proliferation [3]. Another bisphosphorylated metabolite of PI, phosphatidylinositol 4,5-bisphosphate ($PI(4,5)P_2$), serves as a co-factor for plasma membrane ion-channels [4]. Loss of phosphatidylinositol 3,5-bisphosphate ($PI(3,5)P_2$), another bisphosphorylated inositide, leads to neurodegeneration, presumably due to malfunction of membrane trafficking [5]. Another type of polar lipid class, glycosphingolipids, comprises major components of the "lipid raft", a rigid membrane microdomain that regulates transmembrane signal transduction [6,7]. Various glycosphingolipids participate in tumor growth, apoptosis, angiogenesis, invasion, and metastasis [8,9]. Some glycosphingolipids, e.g., GD3, promote tumor growth and metastasis via vascular endothelial growth factor (VEGF) [10], whereas other glycosphingolipids, e.g., Gb3, induce apoptosis in tumor cells [11].

Profiling of natural lipids remains challenging due to their >10,000 combinations of polar head group, glycan composition and branching pattern, and the variation in hydrocarbon chain length and degree of unsaturation/hydroxylation. "Shotgun lipidomics" (namely, direct mass analysis without prior liquid chromatography (LC) separation), can define more than 200 lipid species [12,13]. Separation of lipids by liquid chromatography prior to MS analysis can unambiguously identify several hundred cellular lipid compositions with high sensitivity [14,15]. Fourier transform ion

* Corresponding author. Tel.: +1 850 644 0648; fax: +1 850 644 1366.
** Corresponding author. Tel.: +1 850 644 0529; fax: +1 850 644 1366.
E-mail addresses: emmett@magnet.fsu.edu (M.R. Emmett), marshall@magnet.fsu.edu (A.G. Marshall).
[1] Also a member of the Department of Chemistry and Biochemistry, Florida State University, 95 Chieftain Way, Tallahassee, FL 32306, USA.
[2] Current address: Pfizer Global Research and Development, 10770 Science Center Dr. (CB2), San Diego, CA 92121, USA.

1387-3806/$ – see front matter © 2010 Elsevier B.V. All rights reserved.
doi:10.1016/j.ijms.2010.10.014

cyclotron resonance (FT-ICR) mass spectrometry has been applied in lipid profiling [16–18]. In this paper, we demonstrate how the high mass accuracy and resolution provided by high resolution FT-ICR MS can facilitate compositional analysis of polar lipid mixtures, especially glycosphingolipids and phospholipids.

2. Materials and methods

2.1. Polar lipid extraction

Polar lipids were extracted as previously described [14,19,20]. Briefly, ~2 million cells were extracted with methanol:chloroform (1:1, v:v). The mixture was sonicated for 30 min followed by incubation in a 48 °C water bath overnight. After centrifugation, the supernatant was collected and phase-partitioned with additional chloroform:H_2O (4:11, v:v). The upper aqueous layer was collected, dried, and stored under nitrogen.

2.2. Polar lipid nano-LC–MS

We followed our previously reported nano-liquid chromatography (nLC)–MS procedure for polar lipid separation [14,19,20]. Each nLC–MS experiment consumed approximately 1/50 of the polar lipid extract. Briefly, the polar lipid extract was dissolved in 20%:80% H_2O:methanol containing 10 mM NH_4OAc and separated by nLC (Eksigent 1D system, Livermore, CA). An 80 mm × 50 μm column (New Objective, Woburn, MA) was self-packed with phenyl-hexyl resin (Phenomenex, Torrance, CA). The gradient was 15%:85% to 2%:98% A:B for 15 min and isocratic at 2%:98% A:B for another 12 min (solvent A: 98%:2% H_2O:methanol with 10 mM NH_4OAc; B: 98%:2% methanol:H_2O with 10 mM NH_4OAc) at a flow rate of 500 nL/min. nLC-effluent was analyzed directly by negative-ion micro-electrospray ionization (ESI) [21,22], LTQ 14.5 T FT-ICR MS [23]. For detection of phospholipids and glycosphingolipids, we chose negative-ion micro-electrospray for better *S*/*N* ratio [24]. Automatic gain control (AGC) was set at 3 million ions and precursor ion mass spectra were collected at high mass resolving power ($m/\Delta m_{50\%}$ = 200,000 at m/z 400) and acquisition rate (>1 Hz). Broadband external calibration was carried out with vendor-provided Calmix standard (Thermo Scientific, Waltham, MA), and mass accuracy was typically better than 500 ppb. Data-dependent tandem mass spectrometry of the three most abundant precursor ions by collision-induced dissociation (CID) was performed in the linear ion trap (LTQ) during collection of the ICR time-domain data.

3. Results and discussion

High mass accuracy provides three tools for analysis of polar lipids. First, we can search an experimental mass list against an accurate mass based lipid library. Our current phospholipid database includes >8000 sphingomyelin (SM), cardiolipin (CL), phosphatidylinositol (PI), phosphatidic acid (PA), phosphatidylserine (PS), phosphatidylglycerol (PG), phosphatidylethanolamine (PE), and phosphatidylcholine (PC) (including both diacyl- and lyso-forms) species. Our current glycosphingolipid database includes >4000 GlcCer, LacCer, Gb3, asialo-GM2, asialo-GM1, GM1, GM2, GM3, GD1, GD2, GD3, SGPG, GT1, GQ1, and sulfatides. With the sub-ppm mass accuracy provided by 14.5 T FT-ICR MS, it is usually possible to narrow down to one or a few possible lipid compositions.

Second, for lipids not included in the above databases, multiplication of each mass in Dalton by the factor, 14.00000/14.01565 yields so-called "Kendrick mass".

$$\text{Kendrick mass} = \text{IUPAC mass} \times \left(\frac{14.00000}{14.01565}\right) \quad (1)$$

Lipids otherwise identical in polar head group and degree of unsaturation/hydroxylation but differing in number of CH_2 groups (the mass of CH_2 in Dalton is 14.01565) will have the same Kendrick mass defect [25]:

$$\text{Kendrick mass defect} = \text{nominal Kendrick mass} - \text{exact Kendrick mass} \quad (2)$$

thereby providing a way to recognize members (including new ones) of a lipid family differing only in hydrocarbon chain length [26].

Third, isotopic "fine structure" denotes isotopic variants of species of the same elemental composition and the same nominal mass (e.g., $^{12}C_c{}^1H_h{}^{16}O_o{}^{34}S$ and $^{13}C_2{}^{12}C_{c-2}{}^1H_h{}^{16}O_o{}^{32}S$). Resolution of the $^{34}S_s$ component (and its relative abundance—see below) thus provides independent evidence for the presence (and number of) sulfur atoms in a given lipid. Examples of all three uses of high mass accuracy will now be presented.

3.1. High mass accuracy based lipid library

For analysis of glycosphingolipids (without any adduct), the smallest mass difference between two monoisotopic masses is 7.4 mDa, corresponding to the mass difference between N_2O_2 (59.9960 Da) and $C_2H_4S_1$ (60.0034 Da) [as for GD2 (d18:1/14:0) vs. SGPG (d18:1/26:2)]. However, glycosphingolipids are rarely detected without an adduct, even after liquid chromatography separation. The most common adducts are sodium and acetate (we used ammonium acetate in LC mobile phase). Considering sodium and acetate adducts, the smallest mass difference between two monoisotopic masses becomes 2.4 mDa, corresponding to Na_1H_1 (23.9976 Da) vs. C_2 (24.0000 Da) [as for GM3 (d18:1/22:0) + Na vs. GM3 (d18:1/24:3)]. If elemental compositions including one or two ^{13}C are considered, the smallest mass difference can be 1.6 mDa, corresponding to $^{13}C_2S_1H_2$ (59.9944 Da) vs. N_2O_2 (59.9960 Da) [e.g., SPGP (d18:1/26:3) containing two ^{13}C vs. monoisotopic (i.e., all ^{12}C) GD2 (d18:1/14:0)].

For phospholipids, the smallest mass difference is 5.9 mDa, corresponding to the mass difference between H_4O_5 (84.0059 Da) and C_7 (84.0000 Da) [as for PI (30:0) + 2O and PG (40:10)]. We rarely observe sodium or acetate adduct ions of phospholipids after LC. However, for direct infusion (direct analysis of lipids without prior separation), the previously discussed 2.4 mDa mass difference due to sodium adduct must be considered. If one or two ^{13}C atoms are considered, then the smallest mass difference becomes 1.8 mDa, corresponding to $^{12}C_2{}^{13}C_1N_1$ (51.0064 Da) vs. H_3O_3 (51.0082 Da) [as for PC (40:6) acetate with one ^{13}C vs. monoisotopic PI (38:0)].

Thus, FT-ICR MS can quickly identify possible phospholipid and glycosphingolipid compositions based solely on accurate mass measurement. However, due to the existence of isomers [e.g., PE (40:2) + 2O and PC (36:2) formate, both of which have the same elemental composition, $C_{45}H_{86}N_1O_{10}P_1$], tandem MS is required for unambiguous structural assignment. A representative LC–MS example of GSC11 glioma stem cell polar lipid extract is shown in the supporting information section (Fig. S1—sum of ~550 scans of broadband nano-LC ESI negative-ion 14.5 T FT-ICR mass spectra; Table S1—representative glycosphingolipids and phospholipids identified in GSC11 glioma stem cells).

Table 1
Identified 3-*O*-sulfoglucuronylparaglobosides (SGPG) in GSC11 cells.

Obs. $[M-2H]^{2-}$	Assignment	Elem. composition	Calc. mass	Obs. mass	Error (ppm)[a]	Kendrick mass	KMD
741.3705	SGPG (d18:0/16:0)	$C_{66}H_{120}N_2O_{32}S_1$	1484.7545	1484.7556	0.74	1483.0977	0.902
755.3858	SGPG (d18:0/18:0)	$C_{68}H_{124}N_2O_{32}S_1$	1512.7858	1512.7862	0.26	1511.0970	0.903
740.3626	SGPG (d18:1/16:0)	$C_{66}H_{118}N_2O_{32}S_1$	1482.7388	1482.7398	0.67	1481.0842	0.916
754.3785	SGPG (d18:1/18:0)	$C_{68}H_{122}N_2O_{32}S_1$	1510.7701	1510.7716	0.99	1509.0847	0.915
768.3938	SGPG (d18:1/20:0)	$C_{70}H_{126}N_2O_{32}S_1$	1538.8014	1538.8022	0.52	1537.0840	0.916
782.4097	SGPG (d18:1/22:0)	$C_{72}H_{130}N_2O_{32}S_1$	1566.8327	1566.8340	0.83	1565.0845	0.916
753.3704	SGPG (d18:1/18:1)	$C_{68}H_{120}N_2O_{32}S_1$	1508.7545	1508.7554	0.60	1507.0707	0.929
767.3861	SGPG (d18:1/20:1)	$C_{70}H_{124}N_2O_{32}S_1$	1536.7858	1536.7868	0.65	1535.0708	0.929
781.4016	SGPG (d18:1/22:1)	$C_{72}H_{128}N_2O_{32}S_1$	1564.8171	1564.8178	0.45	1563.0705	0.929
795.4175	SGPG (d18:1/24:1)	$C_{74}H_{132}N_2O_{32}S_1$	1592.8484	1592.8496	0.75	1591.0710	0.929
780.3941	SGPG (d18:1/22:2)	$C_{72}H_{126}N_2O_{32}S_1$	1562.8014	1562.8028	0.90	1561.0578	0.942
794.4097	SGPG (d18:1/24:2)	$C_{74}H_{130}N_2O_{32}S_1$	1590.8327	1590.8340	0.82	1589.0577	0.942
808.4250	SGPG (d18:1/26:2)	$C_{76}H_{134}N_2O_{32}S_1$	1618.8640	1618.8646	0.37	1617.0570	0.943
793.4017	SGPG (d18:1/24:3)	$C_{74}H_{128}N_2O_{32}S_1$	1588.8171	1588.8180	0.57	1587.0439	0.956
807.4175	SGPG (d18:1/26:3)	$C_{76}H_{132}N_2O_{32}S_1$	1616.8484	1616.8496	0.74	1615.0442	0.956
792.3942	SGPG (d18:1/24:4)	$C_{74}H_{126}N_2O_{32}S_1$	1586.8014	1586.8030	1.01	1585.0312	0.969
806.4096	SGPG (d18:1/26:4)	$C_{76}H_{130}N_2O_{32}S_1$	1614.8327	1614.8338	0.68	1613.0307	0.969
791.3863	SGPG (d18:1/24:5)	$C_{74}H_{124}N_2O_{32}S_1$	1584.7858	1584.7872	0.88	1583.0176	0.982
805.4013	SGPG (d18:1/26:5)	$C_{76}H_{128}N_2O_{32}S_1$	1612.8171	1612.8172	0.06	1611.0163	0.984

[a] Mass error after external calibration with Calmix standard (Thermo Scientific, Waltham, MA).

3.2. Kendrick mass defect (KMD)

A major source of variability in fatty acids is hydrocarbon chain length. Because fatty acids elongate by reaction with acetyl-CoA [27], elongated fatty acids differ from their precursor fatty acid by $(CH_2)_{2n}$. Thus, homologous series (species differing only by multiples of $[CH_2]$) share the same Kendrick mass defect and differ in nominal Kendrick mass by a multiple of 14. Thus, lipids can be grouped into different homologous alkylation series, thereby facilitating compositional assignment for higher mass members of the series based on unique assignment for lower-mass members of the same series.

Another type of variability of fatty acid is degree of unsaturation (number of double bonds). Double bonds can be introduced into a fatty acid by desaturase [28]. Addition of one double bond increases the Kendrick mass defect by 0.013. Lipids differing from a given homologous alkylation series only in number of double bonds can then be quickly recognized from Kendrick mass defect increase of 0.013 and Kendrick nominal mass decrease of 2.

Yet another fatty acid modification is oxidation [29]. Addition of one oxygen increases the KMD by 0.023. Therefore, lipids species that differ from a given homologous alkylation series only by oxidation state can be identified from their increase in Kendrick mass defect by 0.023 and nominal Kendrick mass increase of 16.

In the course of analyzing the effect of induced phenotypic differentiation of glioblastoma stem cells [20], we found a series of related lipid species not previously reported in glioblastoma tumor cells. The newly discovered lipids (Table 1) could be identified as 3-*O*-sulfoglucuronylparaglobosides (SGPGs) (Fig. 1). We can easily group SGPGs with the same degree of unsaturation (i.e., same number of double bonds) based on their identical Kendrick mass defect and Kendrick mass increment of 28. For example, SGPG (d18:1/18:1), has a Kendrick mass defect of 0.929, along with SGPGs (d18:1/20:1), (d18:1/22:1) and (d18:1/24:1). SGPGs with the same fatty acid chain lengths but varying degree of unsaturation are readily identified from their Kendrick mass defect increment of 0.013 and Kendrick mass decrease of 2. For example, the Kendrick mass defects for SGPGs (d18:1/24:1), (d18:1/24:2), (d18:1/24:3), (d18:1/24:4) and (d18:1/24:5) are 0.929, 0.942, 0.956, 0.969 and 0.982, with Kendrick mass defect increment of 0.013. Grouping of related SGPGs based on Kendrick mass defect followed by fragmentation of selected related SGPGs eventually enables us to characterize the SGPG structure.

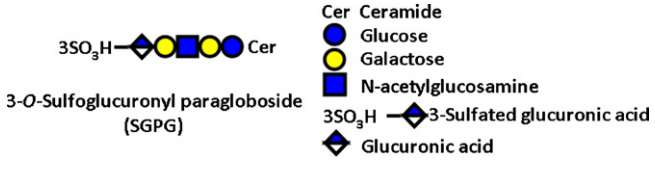

Fig. 1. Structure of novel 3-*O*-sulfoglucuronylparagloboside (SGPG) identified in GSC11 cells.

We previously reported the change of cellular polar lipid profile in response to combined p53 gene/chemo-therapies for U87 glioblastoma cells [14]. The treated U87 cells are more prone to apoptosis [30], and one of the significant changes is a dramatic increase in hydroxylated phospholipids. Kendrick mass defect analysis quickly reveals series of phospholipids with different degrees of hydroxylation. Consider for example phosphatidylinositol lipids (PI) (Table 2), (38:4) (38 total carbons and 4 double bonds in the diacyl chains), (38:4)+O [i.e., (38:4) with one hydroxylation], (38:4)+2O (two hydroxylations), (38:4)+3O (three hydroxylations), and (38:4)+4O (four hydroxylations) with Kendrick mass defects of 0.433, 0.456, 0.480, 0.502, and 0.524 (Kendrick mass defect increment of 0.023) (see Table S2 for a complete list of identified PIs). Polyhydroxylated phospholipids have until now been reported only rarely in mammalian cells. Thus, a database search with limited polyhydroxylation entries may miss some of the polyhydroxylated lipid species that can be easily identified based on Kendrick mass defect.

3.3. Isotopic fine structure

FT-ICR MS can resolve isotopic fine structure as an additional tool for structural identification or verification. In contrast to the monoisotopic (single) peak for which the elemental composition includes only ^1H, ^{12}C, ^{14}N, ^{16}O, and ^{32}S isotopes, signals at successively high nominal mass correspond to multiple combinations of isotopes. For example, ^{34}S vs. $^{13}C_2$, ^{13}C vs. ^{15}N, etc. differ by up to a few mDa. Shi et al. exploited isotopic fine structure for a ^{13}C, ^{15}N doubly depleted p16 (~16 kDa) tumor suppressor protein to determine the number of sulfurs in the protein [31]. Similar sulfur counting has been applied to confirm the elemental composition of petromyzonamine disulfate (PADS) from sea lamprey [32].

Table 2
Representative phosphatidylinositols (PI), especially hydroxylated PI identified in U87 cells treated with combined p53 gene- and chemo-therapies.

PI	Measured mass	Calc. mass	Error (ppm)[a]	Chemical formula	Kendrick mass	KMD
(38:4)	886.5569	886.5572	−0.34	$C_{47}H_{83}O_{13}P_1$	885.567	0.433
(38:4)+O	902.552	902.5521	−0.11	$C_{47}H_{83}O_{14}P_1$	901.5442	0.456
(38:4)+2O	918.546	918.547	−1.09	$C_{47}H_{83}O_{15}P_1$	917.5203	0.480
(38:4)+3O	934.5414	934.5419	−0.54	$C_{47}H_{83}O_{16}P_1$	933.4979	0.502
(38:4)+4O	950.5377	950.5368	0.95	$C_{47}H_{83}O_{17}P_1$	949.4763	0.524

[a] Mass error after external calibration with Calmix standard (Thermo Scientific, Waltham, MA).

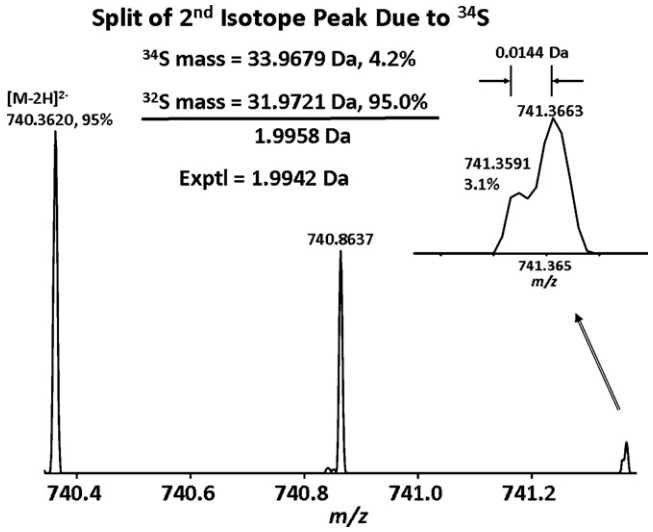

Fig. 2. Isotopic fine structure of SGPG (d18:1/16:0) $[M-2H]^{2-}$, 740.3620 Da. The inset shows the splitting of the second isotope peak due to ^{34}S. The calculated mass difference between ^{34}S and ^{32}S is 1.9958 Da and that observed is 1.9942 Da. The calculated natural abundance of ^{34}S is 4.2% and that observed is 3.1%.

Fig. 2 shows resolution of the ^{34}S component (natural abundance of 4.2%) of SGPG (d18:1/16:0) $[M-2H]^{2-}$ at m/z 740.3620, separated from the monoisotopic peak by 1.9942 Da, in good agreement with the calculated value of 1.9958 Da. The observed mass difference between the ^{34}S and $^{13}C_2$ components is 0.0144 Da. Note that ultrahigh mass resolving power is required to access such isotopic fine structure. The calculated mass difference between ^{34}S and $^{13}C_2$ components is 0.0109 Da. Theoretically, $m/\Delta m_{50\%} = 250{,}000$ (at m/z 400) is required to achieve ^{34}S and $^{13}C_2$ separation at 50% valley (for equal peak heights) for doubly deprotonated ions at m/z 741.36. Thus, our experimental resolving power ($m/\Delta m_{50\%} = 200{,}000$ at m/z 400) barely resolves the ^{34}S and $^{13}C_2$ components. However, higher mass resolving power comes at the expense of slower duty cycle. In future, to further improve mass resolution for on-line LC–MS, we shall employ higher magnetic field while maintaining the same acquisition period. Moreover, the observed relative abundance of 3.1% for the ^{34}S component confirms the presence of only one sulfur (two sulfurs would exhibit a relative abundance of 8.4% for the $^{34}S_2$ component, etc.).

4. Conclusion

Resolution of the smallest mass differences in glycosphingolipids (1.6 mDa) and phospholipids (1.8 mDa), combined with the ultrahigh mass accuracy provided by FT-ICR MS enables quick assignment of phospholipids and glycosphingolipids from an accurate mass based lipid library. Kendrick mass defect analysis is vital for identification and characterization of previously unknown species or species not included in such a library. Finally, resolution of isotopic fine structure reveals the presence (and number) of specific atoms in biological glycosphingolipids (e.g., sulfur).

Acknowledgments

Financial support from the NSF Division of Materials Research through DMR-06-54118, and the State of Florida is gratefully acknowledged. We thank Yongjie Ji and Dr. Howard Colman from M.D. Anderson Cancer Center for providing GSC11 glioblastoma stem cells and U87 glioblastoma cells.

Appendix A. Supplementary data

Supplementary data associated with this article can be found, in the online version, at doi:10.1016/j.ijms.2010.10.014.

References

[1] A.D. Watson, J. Lipid Res. 47 (2006) 2101–2111.
[2] M.R. Wenk, Nat. Rev. Drug Discov. 4 (2005) 594–610.
[3] P.T. Hawkins, K.E. Anderson, K. Davidson, L.R. Stephens, Biochem. Soc. Trans. 34 (2006) 647–662.
[4] B.C. Suh, B. Hille, Annu. Rev. Biophys. 37 (2008) 175–195.
[5] Y. Zhang, S.N. Zolov, C.Y. Chow, S.G. Slutsky, S.C. Richardson, R.C. Piper, B. Yang, J.J. Nau, R.J. Westrick, S.J. Morrison, M.H. Meisler, L.S. Weisman, Proc. Natl. Acad. Sci. U.S.A. 104 (2007) 17518–17523.
[6] D.A. Brown, E. London, Annu. Rev. Cell Dev. Biol. 14 (1998) 111–136.
[7] S. Hakomori, K. Handa, K. Iwabuchi, S. Yamamura, A. Prinetti, Glycobiology 8 (1998), xi–xi10.
[8] S. Hakomori, Cancer Res. 56 (1996) 5309–5318.
[9] R. Kannagi, M. Izawa, T. Koike, K. Miyazaki, N. Kimura, Cancer Sci. 95 (2004) 377–384.
[10] G. Zeng, L. Gao, S. Birklé, R.K. Yu, Cancer Res. 60 (2000) 6670–6676.
[11] M. Mangeney, C.A. Lingwood, S. Taga, B. Caillou, T. Tursz, J. Wiels, Cancer Res. 53 (1993) 5314–5319.
[12] C.S. Ejsing, J.L. Sampaio, V. Surendranath, E. Duchoslav, K. Ekroos, R.W. Klemm, K. Simons, A. Shevchenko, Proc. Natl. Acad. Sci. U.S.A. 106 (2009) 2136–2141.
[13] X. Han, R.W. Gross, Mass Spectrom. Rev. 24 (2005) 367–412.
[14] H. He, C.A. Conrad, C.L. Nilsson, Y. Ji, T.M. Schaub, A.G. Marshall, M.R. Emmett, Anal. Chem. 79 (2007) 8423–8430.
[15] U. Sommer, H. Herscovitz, F.K. Welty, C.E. Costello, J. Lipid Res. 47 (2006) 804–814.
[16] M. Jain, C.J. Petzold, M.W. Schelle, M.D. Leavell, J.D. Mougous, C.R. Bertozzi, J.A. Leary, J.S. Cox, Proc. Natl. Acad. Sci. U.S.A. 104 (2007) 5133–5138.
[17] M.D. Leavell, J.A. Leary, Anal. Chem. 78 (2006) 5497–5503.
[18] L.A.J. Lerno, J.B. German, C.B. Lebrilla, Anal. Chem. 82 (2010) 4236–4245.
[19] H. He, C.L. Nilsson, M.R. Emmett, Y. Ji, A.G. Marshall, R.A. Kroes, M. Schmidt, J.R. Moskal, H. Colman, F.F. Lang, C.A. Conrad, Glycoconjug. J. 27 (2010) 27–38.
[20] H. He, C.L. Nilsson, M.R. Emmett, A.G. Marshall, R.A. Kroes, J.R. Moskal, Y. Ji, H. Colman, W. Priebe, F.F. Lang, C.A. Conrad, J. Proteome Res. 9 (2010) 2098–2108.
[21] M.R. Emmett, R.M. Caprioli, J. Am. Soc. Mass Spectrom. 5 (1994) 605–613.
[22] M.R. Emmett, F.M. White, C.L. Hendrickson, S.D. Shi, A.G. Marshall, J. Am. Soc. Mass Spectrom. 9 (1998) 333–340.
[23] T.M. Schaub, C.L. Hendrickson, S. Horning, J.P. Quinn, M.W. Senko, A.G. Marshall, Anal. Chem. 80 (2008) 3985–3990.
[24] S.B. Levery, Methods Enzym. 405 (2005) 300–369.
[25] E. Kendrick, Anal. Chem. 35 (1963) 2146.
[26] C.A. Hughey, C.L. Hendrickson, R.P. Rodgers, A.G. Marshall, K. Qian, Anal. Chem. 73 (2001) 4676–4681.
[27] D.L. Cinti, L. Cook, M.N. Nagi, S.K. Suneja, Prog. Lipid Res. 31 (1992) 1–51.
[28] J. Shanklin, E.B. Cahoon, Annu. Rev. Plant Physiol. Plant Mol. Biol. 49 (1998) 611–641.
[29] E.N. Frankel, Lipid Oxidation, The Oily Press, 2005.
[30] M. Puchades, C.L. Nilsson, M.R. Emmett, K.D. Aldape, Y. Ji, F.F. Lang, T.J. Liu, C.A. Conrad, J. Proteome Res. 6 (2007) 869–875.
[31] D.-H. Shi, C.L. Hendrickson, A.G. Marshall, Proc. Natl. Acad. Sci. U.S.A. 95 (1998) 11532–11537.
[32] T.R. Hoye, V. Dvornikovs, J.M. Fine, K.R. Anderson, C.S. Jeffrey, D.C. Muddiman, F. Shao, P.W. Sorensen, J. Wang, J. Org. Chem. 72 (2007) 7544–7550.